






## Niosome-based delivery systems for olanzapine: Formulation, characterisation, and kinetic evaluation

SAMIAH ALHABARDI<sup>1,\*</sup>   
BASMALH ALDOSARI<sup>1</sup>   
GADAH AL-HAMOUD<sup>2</sup>   
SHOG MOAHMMED ALALI<sup>1</sup>  
REEMA AL KHBIAH<sup>1</sup>  
LAMA ALBULAYHI<sup>1</sup>  
WEDAD SARAWI<sup>3</sup>   
NAIFA ALENAZI<sup>4</sup> 

<sup>1</sup> Department of Pharmaceutics  
College of Pharmacy, King Saud  
University, Riyadh, Saudi Arabia

<sup>2</sup> Department of Pharmacognosy  
College of Pharmacy, King Saud  
University, Riyadh, Saudi Arabia

<sup>3</sup> Department of Pharmacology and  
Toxicology, College of Pharmacy  
King Saud University, P.O. Box  
22452, Riyadh 11495, Saudi Arabia

<sup>4</sup> College of Pharmacy, Princess  
Nourah bint Abdulrahman  
University, Riyadh, Saudi Arabia

Accepted July 25, 2025  
Published online July 26, 2025

### ABSTRACT

This study investigates the development and characterisation of niosome-based delivery systems for olanzapine, an antipsychotic drug. Niosomes were prepared using various grades of Span surfactants (Span 60, Span 40, and Span 20) in combination with cholesterol at different ratios. The formulations were characterised in terms of particle size, polydispersity index, zeta potential, and encapsulation efficiency. Results showed an inverse relationship between surfactant hydrophilic-lipophilic balance (HLB) values and niosome size, with Span 60 producing the smallest vesicles. Optimal formulations were achieved with a 1:1 ratio of surfactant to cholesterol. Span 60 niosomes exhibited the highest encapsulation efficiency (up to  $81 \pm 2.5\%$ ) and the most negative zeta potential, indicating superior stability. *In vitro* release studies demonstrated sustained release profiles for all niosomal formulations compared to the free drug, with Span 60 formulations showing the slowest release rates. Release kinetics analysis revealed a Fickian diffusion-controlled mechanism best described by the Korsmeyer-Peppas model. These findings suggest that niosomal formulations, particularly those based on Span 60, offer a promising approach for improving olanzapine delivery, potentially enhancing its bioavailability and therapeutic efficacy in the treatment of psychiatric disorders.

**Keywords:** niosome, olanzapine, physicochemical characterisation, kinetic evaluation

### INTRODUCTION

Olanzapine, an antipsychotic of the thienobenzodiazepine class, is widely used in the treatment of schizophrenia and related psychiatric disorders. It is classified as an “atypical antipsychotic” (also known as a second-generation antipsychotic) because, unlike older typical antipsychotics, it blocks both dopamine and serotonin receptors and is associated with a lower risk of movement-related side effects, such as tremors and muscle stiffness. Its effectiveness stems from its unique pharmacological profile, primarily antagonising

---

\* Correspondence; e-mail: salhabardi@ksu.edu.sa

dopamine D2 and serotonin 5-HT<sub>2A</sub> receptors, with a higher affinity for the latter. This dual action allows olanzapine to manage both positive and negative symptoms of psychosis effectively (1). Unlike traditional antipsychotics, olanzapine's weaker binding to D2 receptors results in a reduced risk of extrapyramidal side effects, a significant advantage in long-term treatment. The drug's broad receptor binding profile, which includes interactions with histamine H<sub>1</sub>, muscarinic M<sub>1-5</sub>, and alpha-1 adrenergic receptors, further enhances its therapeutic potential (2). These pharmacological properties, combined with its improved side effect profile compared to first-generation antipsychotics, have established olanzapine as a valuable and widely prescribed option in psychiatric care (3). Due to pharmacokinetic problems, olanzapine's efficacy is restricted, despite its therapeutic advantages. Its oral bioavailability is approximately 60 %, primarily due to extensive first-pass metabolism in the liver, which limits the amount of drug that reaches systemic circulation. Additionally, olanzapine exhibits poor aqueous solubility (0.076 mg mL<sup>-1</sup> at neutral pH) and moderate lipophilicity (log $P$  = 1.8), but its solubility increases significantly in acidic and organic solvents such as HCl (16.56 mg mL<sup>-1</sup>), DMSO (62 mg mL<sup>-1</sup>), and ethanol (9 mg mL<sup>-1</sup>) (4). The drug has a large volume of distribution, around 1000 litres, indicating extensive tissue distribution, and is highly protein-bound, with about 93 % attached to plasma proteins such as albumin and alpha-1 acid glycoprotein. This high protein binding limits the free drug available to cross the blood-brain barrier, resulting in only a modest effective dose reaching the brain, where it exerts its primary therapeutic effects (5).

Given the limitations of olanzapine's bioavailability, there is increasing interest in novel drug delivery systems, particularly niosomes (6). Niosomes are microscopic, lamellar vesicles primarily composed of non-ionic surfactants and cholesterol. The non-ionic surfactants, such as Spans and Tweens/Polysorbates, possess both hydrophilic (water-attracting) head groups and hydrophobic (water-repelling) tail groups (7). In aqueous environments, surfactant molecules self-assemble such that the hydrophilic heads face the aqueous phase (both inside and outside the vesicle), while the hydrophobic tails align inward, forming a closed bilayer structure. Cholesterol is incorporated into the bilayer to provide rigidity and stability, reducing membrane permeability and preventing leakage of encapsulated drugs. This bilayer configuration allows niosomes to encapsulate both hydrophilic drugs (in the aqueous core) and lipophilic drugs (within the bilayer itself). Energy input (*e.g.*, heat or agitation) is typically required for vesicle formation. The resulting structure is similar to liposomes, but generally more stable due to the use of non-ionic surfactants (8).

This delivery system has the potential to improve absorption and bioavailability, leading to better therapeutic outcomes and fewer side effects (9). Niosomes are appealing due to their stability, biodegradability, and biocompatibility, making them suitable for pharmaceutical applications without triggering an immune response (10). They also provide protection against environmental factors and biological enzymes, which is especially beneficial for drugs administered orally or parenterally (11). Furthermore, the cost-effectiveness of niosomes, derived from inexpensive non-ionic surfactants, positions them as an attractive option for researchers and pharmaceutical companies aiming to develop innovative drug formulations (12). Overall, niosomes represent a promising approach to overcoming the pharmacokinetic challenges associated with olanzapine, potentially improving its clinical efficacy and patient compliance (10).

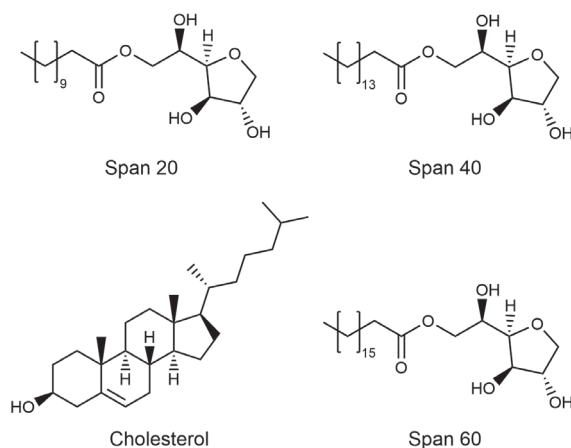


Fig. 1. Chemical structure of different grades of Span and cholesterol.

The present study focuses on the development of olanzapine-loaded niosomes as drug carriers by systematically investigating the effects of various Span surfactant grades (Fig. 1) and cholesterol ratios, an aspect previously underexplored in the literature (13). By optimising surfactant composition and formulation conditions specifically for olanzapine, this work not only advances understanding of niosomal stability and performance but also addresses key limitations of the drug, such as poor water solubility and bioavailability.

## EXPERIMENTAL

### Materials

Olanzapine powder (free base, purity  $\geq 99\%$ , Jazeera JPI, Riyadh, Saudi Arabia) was used. Span 60 (purity  $\geq 99\%$ ), Span 40 (purity  $\geq 98\%$ ), Span 20 (purity  $\geq 99\%$ ) and cholesterol (purity  $\geq 99\%$ ) were purchased from Wako Pure Chemical Industries Ltd., Japan) were utilised as primary components for niosome preparation. Diethyl ether (analytical grade, Merck Chemical Company, Germany) was employed as the organic solvent. Phosphate-buffered saline (PBS, pH 7.4, Sigma-Aldrich, USA) and Polysorbate 20 (purity  $\geq 99\%$ , Sigma-Aldrich) were used for *in vitro* release studies. Phosphotungstic acid (Sigma-Aldrich) was used for negative staining in TEM analysis. Polyvinylidene fluoride (PVDF) syringe filters (0.22  $\mu\text{m}$ , Millipore, USA) were used for sample filtration. All other chemicals and reagents (analytical grade, Merck Chemical Company) were employed as received without further purification.

### Methods

*Ether injection method.* – Niosomes were prepared using the ether injection method. Specifically, Span 60, Span 40, Span 20, and cholesterol were used as the primary components. The required amounts of surfactant and cholesterol were first dissolved in 10 mL of

diethyl ether (Table I). Olanzapine was then added to this lipid solution. The resulting lipid-drug solution was slowly injected at a rate of 0.25 mL min<sup>-1</sup> into 10 mL of preheated phosphate-buffered saline (PBS, pH 7.4) maintained at 60 ± 2 °C using a 14-gauge needle. The mixture was stirred continuously at 50 rpm with a magnetic stirrer (IKA RCT basic, Germany) during injection to ensure uniform vesicle formation.

As the ether rapidly vaporised upon contact with the hot aqueous phase, niosomes spontaneously formed due to the self-assembly of the surfactant and cholesterol molecules into bilayer vesicles. After injection, the suspension was stirred at 50 rpm for 2 hours at 60 °C to ensure complete evaporation of residual diethyl ether (boiling point: 34.6 °C). The niosomal suspension was then allowed to equilibrate at 25 ± 2 °C for 30 minutes and subsequently stored at 4–8 °C until further characterisation.

Table I. Surfactant and cholesterol composition for olanzapine encapsulated niosomes

Formulation code	Composition	Molar ratio	Surfactant (mg)	Cholesterol (mg)	Olanzapine (mg)
FS60-1	Cholesterol : Span 60	1:1	100	100	10
FS60-2	Cholesterol : Span 60	1:2	133	67	10
FS60-3	Cholesterol : Span 60	1:3	150	50	10
FS60-4	Cholesterol : Span 60	1:4	160	40	10
FS40-1	Cholesterol : Span 40	1:1	100	100	10
FS40-2	Cholesterol : Span 40	1:2	133	67	10
FS40-3	Cholesterol : Span 40	1:3	150	50	10
FS40-4	Cholesterol : Span 40	1:4	160	40	10
FS20-1	Cholesterol : Span 20	1:1	100	100	10
FS20-2	Cholesterol : Span 20	1:2	133	67	10
FS20-3	Cholesterol : Span 20	1:3	150	50	10
FS20-4	Cholesterol : Span 20	1:4	160	40	10

### Characterisation of niosomes

*Determination of vesicle size, polydispersity index and zeta potential.* – Particle size, polydispersity index (PDI), and zeta potential of the niosomes were analysed using a Zetasizer Nano ZS (Malvern Panalytical, UK) equipped with dynamic light scattering (DLS) and laser Doppler electrophoresis technologies. For particle size and PDI measurements, 1 mL of niosomal suspension was diluted 1:10 (V/V) with deionised water to ensure optimal scattering intensity and avoid multiple scattering effects. The diluted samples were analysed in triplicate at 25 °C using a 633 nm He-Ne laser and a detector angle of 173 °, with data processed *via* cumulant analysis to determine the Z-average hydrodynamic diameter and PDI.

Zeta potential measurements were performed using the same instrument, with samples diluted similarly, to maintain electrophoretic mobility within the instrument's detec-

tion range. The electrophoretic mobility of the niosomes was converted to potential using the Smoluchowski approximation, and triplicate measurements were conducted at 25 °C to ensure reproducibility. Zeta potential measurements in deionised water (ionic strength  $\approx 0$ ) provide a baseline for inter-formulation stability comparisons. While PBS (pH 7.4, ionic strength  $\approx 0.16 \text{ mol L}^{-1}$ ) may reduce absolute zeta potential values through charge shielding, prior studies confirm that relative trends between Span-based niosomes remain consistent across media (14).

*Determination of the drug entrapment efficiency in niosomes.* – The entrapment efficiency (EE %) of niosomes was quantified using an ultracentrifugation method coupled with UV-Vis spectrophotometry. An aliquot of niosomal suspension (1 mL) was diluted 1:10 (V/V) with PBS, pH 7.4 containing 0.5 % (m/V) Polysorbate 20 to ensure uniform dispersion and enhance olanzapine solubility. The diluted sample was ultracentrifuged at 17,000 rpm (25,000  $\times g$ ) for 45 minutes at 4 °C to sediment vesicles, leaving free drug in the supernatant. After ultracentrifugation, the supernatant was carefully aspirated and filtered through a 0.22  $\mu\text{m}$  membrane to remove residual particulates.

The absorbance of the supernatant was measured at 206 nm using a UV-Vis spectrophotometer. For quantification, a standard calibration curve was prepared by dissolving olanzapine in PBS (pH 7.4) with 0.5 % (m/V) Polysorbate 20, followed by serial dilution to achieve concentrations within the linear range. The curve exhibited excellent linearity ( $R^2 = 0.998$ ). The concentration of untrapped drug was calculated using the equation:

$$EE \% = \frac{c_{\text{total}} - c_{\text{free}}}{c_{\text{total}}} \times 100$$

where  $c_{\text{total}}$  is the initial drug concentration (10 mg mL<sup>-1</sup>) and  $c_{\text{free}}$  is the free drug concentration quantified in the supernatant. Triplicate measurements ensured reproducibility, with results reported as mean  $\pm$  SD.

*In vitro* release studies. – The *in vitro* release profiles of optimised niosomal formulations were evaluated using Franz diffusion cells (12 mL). The *in vitro* release was conducted using PBS, pH 7.4 containing 0.5 % (m/V) Polysorbate 20 as the receptor medium, maintained at  $37 \pm 0.5$  °C and continuously stirred.

In the donor compartment, 2 mL of niosomal suspension or the drug suspension in PBS (corresponding to olanzapine content in niosomes) was applied. Aliquots (0.5 mL) were withdrawn from the receptor chamber at 1, 2, 4, 6, 8, 12, and 24 hours, with immediate replacement by fresh pre-warmed medium to maintain constant volume and sink conditions. Samples were filtered through 0.22  $\mu\text{m}$  PVDF syringe filters before analysis.

A calibration curve was constructed using olanzapine standards (2.5–25  $\mu\text{g mL}^{-1}$  in PBS, pH 7.4, containing 0.5 % (m/V) Polysorbate 20). A stock solution (100  $\mu\text{g mL}^{-1}$ ) was serially diluted, and absorbance was measured at 206 nm (Shimadzu UV-1900i). The curve exhibited linearity ( $R^2 = 0.9993$ ) across the tested range.

*Kinetics of drug release.* – The drug release profiles from niosomes were analysed using the DD-Solver add-in for Microsoft Excel to systematically assess the release mechanisms. Release data were fitted to four pharmacokinetic models: Zero-order (constant rate), First-order (concentration-dependent), Higuchi (diffusion-controlled), and Korsmeyer-Peppas

(transport mechanism). The coefficient of determination ( $R^2$ ) was computed for each model to evaluate the fit quality, with the highest  $R^2$  value indicating the most appropriate model for describing the release behaviour. This approach provided insights into whether drug release was governed by diffusion, matrix erosion, or a combination of mechanisms.

*In vitro stability study.* – The *in vitro* stability of selected olanzapine niosomes was evaluated over six months under refrigerated storage (4–8 °C). Formulations (FS60-1 to FS60-4 and FS40-1 to FS40-4) were stored in light-protected vials, with samples analysed at 3 and 6 months. Key parameters: vesicle size, PDI, zeta potential, and EE % were assessed using dynamic light scattering (Malvern Zetasizer Nano ZS) for size/PDI, electrophoretic mobility for zeta potential, and UV-Vis spectrophotometry (after ultracentrifugation) for EE %. Triplicate measurements ensured reproducibility, and one-way ANOVA ( $p < 0.05$ ) provided statistical rigour. This approach systematically quantified colloidal stability and drug retention during storage.

### Statistical analysis

The study compared different niosomal formulations and evaluated their key properties using statistical analysis. One-way ANOVA was used for comparing more than two groups, while the independent samples *t*-test was employed for direct two-group comparisons. Statistical significance was set at  $p < 0.05$ , meaning differences were considered significant if the probability of random occurrence was below this threshold. Results were reported as mean  $\pm$  standard deviation, with all measurements performed in triplicate for accuracy and reproducibility. Data analysis was carried out using SPSS 10.1 for Windows, allowing thorough statistical evaluation of the experimental outcomes.

## RESULTS AND DISCUSSION

### Preparation and characterisation of niosomes

This study focused on optimising olanzapine niosome formulations by examining the effects of different surfactant types and ratios on key characteristics. The ether injection method was used to create various niosome formulations, systematically altering surfactant parameters to identify the optimal combination (15). During the study, a variety of niosome formulations were prepared using the ether injection technique. The formulations are categorised into three main groups: FS60, FS40, and FS20, corresponding to Span 60, Span 40, and Span 20 surfactants, respectively. Span 60 is a nonionic surfactant synthesised by the esterification of sorbitan with stearic acid. Span 40 is a sorbitan ester derived from the combination of sorbitan and palmitic acid. Similarly, Span 20 is produced from sorbitan and lauric acid. Generally, Spans are sorbitan fatty acid esters, which are commonly used as emulsifiers and stabilisers in pharmaceutical formulations (16). Each group of niosomes is further divided based on cholesterol-to-surfactant ratios, as shown before in Table I.

The results presented in Table II offer valuable insights into olanzapine-encapsulated niosomes' main characteristics, including particle size, PDI, zeta potential, and EE %.

Olanzapine niosomes revealed a wide range of mean particle diameters, from  $112 \pm 4$  to  $651 \pm 22$  nm (Table II). Statistical analysis using one-way ANOVA demonstrated a

significant difference in particle size between the different surfactant groups ( $p < 0.05$ ). Also, this study showed a significant correlation between surfactant (HLB) values and niosome size ( $p < 0.05$ ). Lower HLB surfactants consistently produced smaller vesicles when cholesterol content remained constant, with FS60 niosomes (lowest HLB) being the smallest, followed by FS40 and FS20 niosomes. Vesicle size increased as the surfactant ratio increased and the cholesterol ratio decreased, with an optimal surfactant-to-cholesterol ratio of 1:1 observed across all formulations. PDI values indicated relatively uniform size distributions in most formulations, with Span 40 niosomes exhibiting lower PDI values, suggesting more homogeneous vesicle populations. The difference in PDI between the examined niosomes was statistically significant ( $p < 0.05$ ).

The zeta potential measurements, which serve as a crucial indicator of niosomes' stability, exhibited a consistent trend across the formulations, mirroring the pattern observed in particle size analysis. All formulations displayed negative zeta potentials, with values ranging from  $-9 \pm 2.5$  to  $-37 \pm 2.8$  mV. Among the formulations, FS60 niosomes demonstrated the most negative zeta potential values, followed by FS40 niosomes, and then FS20 niosomes. Statistical analysis confirmed significant differences in zeta potential between the groups (one-way ANOVA,  $p < 0.01$ ), with FS60 niosomes demonstrating the most negative zeta potential values, followed by FS40 niosomes, and then FS20 niosomes.

The analysis of EE % in niosomal formulations reveals a relationship between surfactant composition, cholesterol content, and vesicle size. As the ratio of surfactant to cholesterol increases within each surfactant group, a general trend of decreasing EE % is observed. However, formulations with higher cholesterol content tend to demonstrate enhanced EE %, particularly in Span 40 and Span 60 formulations. A distinct pattern emerges in EE %, with FS60 niosomes exhibiting the highest value at 81 %, followed by FS40 at 66 %, and FS20 at 29 %. These differences in EE % were statistically significant (one-way ANOVA,  $p < 0.001$ ). This trend highlights the superior encapsulation performance of Span 60 formulations. Notably, an inverse correlation is observed between entrapment efficiency and vesicle size (Pearson's  $r = -0.85$ ,  $p < 0.01$ ), suggesting that smaller vesicles are more adept at encapsulating olanzapine. This unexpected relationship between vesicle size and encapsulation efficiency underscores the complex interplay of factors influencing the drug entrapment capabilities of niosomes.

The selection of surfactant and its proportion relative to cholesterol plays a pivotal role in determining the physicochemical properties of niosomes (17). Our study revealed an inverse relationship between the HLB value of surfactants and niosome size, with Span 60 (HLB 4.7) consistently producing smaller vesicles compared to Span 40 (HLB 6.7) and Span 20 (HLB 8.6). Previous studies demonstrated a correlation between surfactant HLB values and niosome particle size (18). Surfactants with lower HLB values, such as Span 60 and Brij 72 (HLB  $\approx 4.8$ ), typically produced smaller niosomes compared to those with higher HLB values, like Tween 60 (HLB = 14.9). This trend is supported by studies on various drug-loaded niosomes, including carvedilol-niosomes and griseofulvin-loaded niosomes. Cholesterol content emerged as another critical factor in niosome formation and stability, with optimal formulations achieved at a 1:1 surfactant-to-cholesterol ratio across all surfactant types, supporting cholesterol's role as a stabilising agent in niosomal membranes (19). The impact of cholesterol content on niosome size appears to be surfactant-dependent; hydrophilic surfactants like Tween 60 show minimal size changes with increas-



ing cholesterol content, whereas more lipophilic surfactants like Brij 72 and Span 60 exhibit decreased average particle diameters at higher cholesterol concentrations (20).

The EE % showed a clear trend, with Span 60 formulations exhibiting the highest EE % (up to  $81 \pm 2.5$  %), followed by Span 40 and Span 20. This superior performance of Span 60 can be attributed to its lower HLB value and longer alkyl chain length, which promote stronger interactions with cholesterol and more efficient drug entrapment (21). The inverse relationship observed between vesicle size and EE % suggests that smaller vesicles may provide a more favourable environment for olanzapine encapsulation, possibly due to increased surface area to volume ratio (22). Zeta potential measurements revealed negative values for all formulations, with Span 60 niosomes showing the most negative zeta potentials. This characteristic is crucial for niosome stability, as it indicates strong electrostatic repulsion between vesicles, preventing aggregation.

Table II. Characteristics of olanzapine niosomes

Formulation code	Particle size (nm)	PDI	Zeta potential (mV)	EE %
FS60-1	$112 \pm 4$	$0.31 \pm 0.04$	$-24 \pm 1.6$	$81 \pm 2.5$
FS60-2	$143 \pm 3.5$	$0.32 \pm 0.02$	$-27 \pm 1.7$	$76 \pm 1.5$
FS60-3	$157 \pm 2.5$	$0.43 \pm 0.01$	$-33 \pm 2.2$	$72 \pm 2.6$
FS60-4	$168 \pm 9.1$	$0.38 \pm 0.06$	$-37 \pm 2.8$	$70 \pm 2.5$
FS40-1	$180 \pm 18$	$0.25 \pm 0.03$	$-22 \pm 4$	$66 \pm 3.5$
FS40-2	$220 \pm 5.5$	$0.20 \pm 0.08$	$-24 \pm 4.6$	$54 \pm 4$
FS40-3	$270 \pm 5.2$	$0.22 \pm 0.03$	$-28 \pm 2.2$	$49 \pm 2$
FS40-4	$310 \pm 30$	$0.27 \pm 0.07$	$-32 \pm 2.6$	$43 \pm 2.3$
FS20-1	$350 \pm 25$	$0.37 \pm 0.02$	$-9 \pm 2.5$	$29 \pm 2.6$
FS20-2	$400 \pm 6$	$0.42 \pm 0.02$	$-11 \pm 2.5$	$27 \pm 1$
FS20-3	$462 \pm 12$	$0.29 \pm 0.04$	$-18 \pm 1.9$	$22 \pm 1.5$
FS20-4	$651 \pm 22$	$0.55 \pm 0.07$	$-21 \pm 3$	$18 \pm 2.5$

The results are expressed as mean  $\pm$  SD,  $n = 3$ .

### In vitro release studies

Niosomes were prepared using the ether injection method, employing surfactants such as Span 20, Span 40, and Span 60 in combination with cholesterol at various ratios. The optimal niosomal formulations for each surfactant were selected based on key characteristics, including size distribution, PDI, zeta potential, and EE %. These selected formulations were then subjected to further *in vitro* release and stability studies to evaluate their performance and suitability for drug delivery applications.

In the present study, the formulations containing Span 20 were withdrawn from further *in vitro* release study due to their low encapsulation efficiency. The *in vitro* release



studies for niosomal formulations containing Span 60 and Span 40, as well as an olanzapine suspension, over a 24-hour period, were conducted in PBS, pH 7.4, containing 0.5 % (*m/V*) Polysorbate 20. The free drug, used as a control, demonstrated the fastest release profile among all tested formulations. It reached 94 % release at 24 hours, indicating that the niosomal formulations effectively sustained the drug release compared to the free drug (Figs. 3 and 4).

For Span 60 formulations, four different niosomal preparations (FS60-1 to FS60-4) were tested. The data shows a gradual increase in drug release over time for all formulations. FS60-1 demonstrated the highest release rate, reaching 82 % at 24 hours, followed by FS60-2 at 62 %, FS60-3 at 52 %, and FS60-4 at 42 %. This trend suggests that the formulation components for FS60-1 resulted in faster drug release compared to the other Span 60 niosomes (Fig. 2). The observation that a 1:1, cholesterol to Span ratio, led to a faster release than a 1:4 ratio appears counterintuitive, as higher cholesterol content is generally expected to increase membrane rigidity and slow drug release. However, this can be explained by considering vesicle size. Namely, smaller vesicles (associated with higher cholesterol) have a larger surface area-to-volume ratio, which may facilitate faster drug release despite increased rigidity. Additionally, excessive cholesterol can disrupt the optimal packing of surfactant molecules, increasing permeability and thus accelerating release (23).

Similarly, for Span 40 formulations, four niosomal preparations (FS40-1 to FS40-4) were evaluated. The release profiles for Span 40 niosomes showed a generally faster release rate compared to Span 60 formulations. FS40-1 and FS40-2 exhibited the highest release rates, both reaching around 82–83 % at 24 hours. FS40-3 and FS40-4 showed lower release rates of 72 and 62 % at 24 hours, respectively (Fig. 3). These results suggest that both Span 60 and Span 40 niosomal formulations can provide sustained release of olanzapine compared to the free drug. However, Span 60 formulations generally showed slower release rates than Span 40 formulations, indicating that Span 60 may be more effective in creating stable niosomes for prolonged drug delivery.

The selected niosomal formulations (FS60-1 to FS60-4) were also examined for olanzapine release kinetics (Tables III and IV) using various mathematical models. The Zero-order model showed varying degrees of fit, with FS60-4 demonstrating the best correlation ( $R^2 = 0.940$ ). The First-order model yielded mixed results, with FS60-2 showing a poor fit (negative  $R^2$  value). The Higuchi model, describing diffusion-based release, showed good correlation for FS60-4 ( $R^2 = 0.946$ ), suggesting a primarily diffusion-controlled release. However, the Korsmeyer-Peppas model emerged as the most suitable for all formulations, with consistently high  $R^2$  values (0.965) and  $n$  values of 0.356, indicating Fickian diffusion-controlled release.

The kinetic analysis of drug release from formulations FS40-1 to FS40-4 revealed varying model fits (Table IV). Zero-order and first-order models showed poor correlation, while the Higuchi model demonstrated better alignment with release kinetics. The Korsmeyer-Peppas model emerged as the most suitable, with the highest  $R^2$  values and  $n$  values below 0.45, indicating a Fickian diffusion-controlled release mechanism.

The release kinetics analysis revealed that olanzapine release from niosomes followed the Korsmeyer-Peppas model, with all formulations exhibiting  $n$ -values  $< 0.45$  (Tables III and IV). For spherical systems like niosomes, these  $n$ -values  $\leq 0.45$  confirm Fickian diffusion, where drug release is driven by passive diffusion through the niosomal matrix, without significant matrix erosion or relaxation. The consistent  $n$ -values and high model fit ( $R^2$ )

underscore the niosomes' structural integrity during release, enabling a sustained, diffusion-controlled profile. These results highlight the formulations' suitability for controlled-release applications, aligning with their stable colloidal properties and predictable release kinetics (24, 25).

Span 60 formulations exhibited slower release rates than Span 40, attributed to Span 60's higher phase transition temperature and greater lipophilicity, resulting in more tightly packed and rigid bilayers (13). The inclusion of cholesterol further reduced drug release rates by enhancing bilayer stability and rigidity (26). These findings highlight the complex

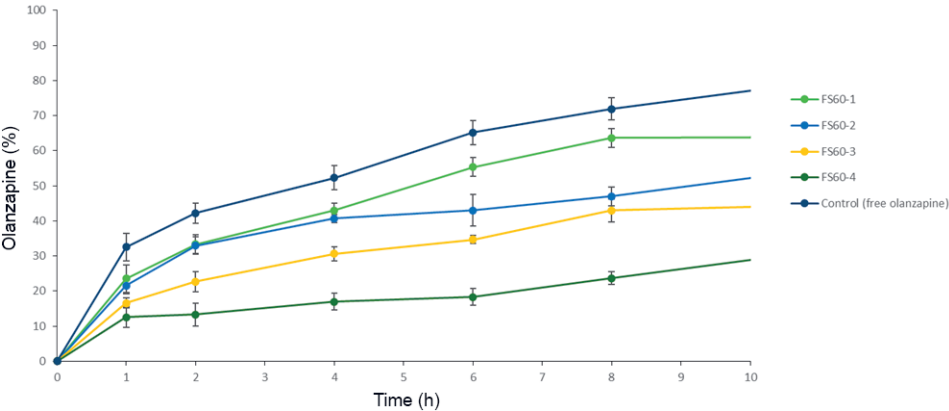


Fig. 2. *In vitro* release profiles of olanzapine Span 60 niosomes. The results are presented as the mean  $\pm$  SD,  $n = 3$ .

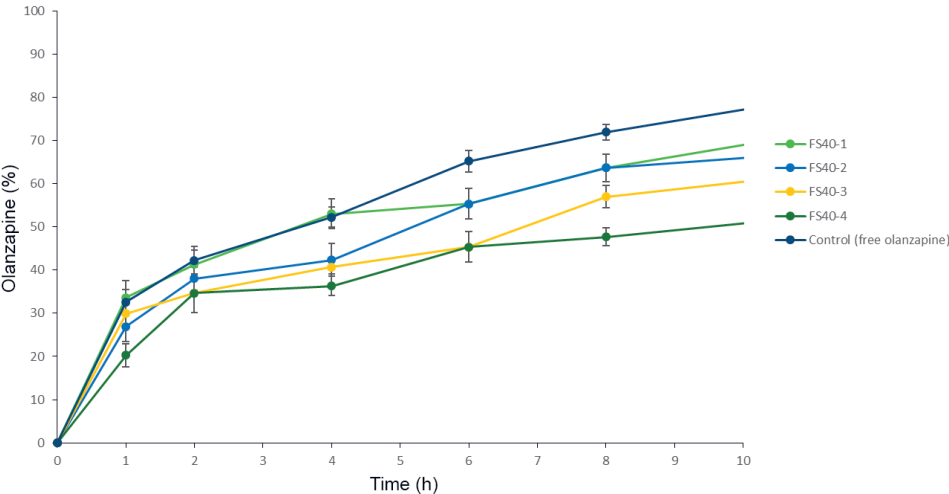


Fig. 3. *In vitro* release profiles of olanzapine Span 40 niosomes. The results are presented as the mean  $\pm$  SD,  $n = 3$ .

interplay between surfactant properties and cholesterol content in determining niosome characteristics, including size, stability, and drug release kinetics (27). The superior performance of Span 60-based niosomes in retarding drug release underscores their potential for improving the delivery and bioavailability of poorly water-soluble drugs like olanzapine through sustained and controlled release mechanisms (28, 29).

Table III. Drug release kinetics of Span 60 niosomes formulation

Formulation code	Zero-order		First-order		Higuchi model	Korsmeyer-Peppas model	
	$R^0$	$R^2$	$R^1$	$R^2$	$R^2$	$n$	$R^2$
FS60-1	4.573	0.826	0.122	0.740	0.844	0.356	0.965
FS60-2	3.646	0.784	0.079	−0.106	0.577	0.356	0.965
FS60-3	3.009	0.787	0.053	0.030	0.765	0.356	0.965
FS60-4	2.174	0.940	0.029	0.618	0.946	0.356	0.965

Table IV. Drug release kinetics of Span 40 niosomes formulation

Formulation code	Zero-order		First-order		Higuchi model	Korsmeyer-Peppas model	
	$R^0$	$R^2$	$R^1$	$R^2$	$R^2$	$n$	$R^2$
FS40-1	4.799	−2.172	0.15233	0.4147	0.5164	0.2803	0.9787
FS40-2	4.675	−0.882	0.13040	0.6861	0.8018	0.3382	0.9755
FS40-3	4.152	−1.612	0.10299	0.2357	0.6369	0.3008	0.9640
FS40-4	3.6036	−1.722	0.07723	−0.1067	0.5920	0.2940	0.9517

### In vitro stability study

Over a 6-month storage period at 4–8 °C, olanzapine-loaded niosomal formulations based on Span 60 and Span 40 displayed distinct stability profiles, with several parameters demonstrating changes typical of niosomal systems (Table V). For Span 60 formulations (FS60-1 to FS60-4), a marked and statistically significant increase in vesicle size was observed over time. For example, the vesicle size of FS60-1 increased from  $112 \pm 4$  nm at time 0 to  $221.7 \pm 6$  nm after 6 months (paired *t*-test,  $p < 0.001$ ), suggesting vesicle aggregation or fusion during storage. Despite this increase, the PDI remained below 0.4, suggesting that the dispersions retained acceptable homogeneity. Zeta potential values for Span 60 niosomes became significantly more negative after 3 months, which may reflect enhanced colloidal stability, before partially reverting at 6 months. EE % in Span 60 niosomes showed a gradual but statistically significant decline, consistent with minor drug leakage, a common finding in niosomal stability studies.

In contrast, Span 40 formulations (FS40-1 to FS40-4) exhibited greater variability. While FS40-1 and FS40-2 showed steady increases in vesicle size, FS40-3 and FS40-4 dis-

played an initial decrease at 3 months, followed by regrowth, a phenomenon sometimes attributed to vesicle compaction or bilayer restructuring. Zeta potential values for Span 40 niosomes trended toward less negative values over time (*e.g.*, FS40-4:  $-32 \pm 2.6$  mV at time 0 to  $-24.6 \pm 1.9$  mV at 6 months;  $p < 0.01$ ), indicating a reduction in electrostatic stabilisation and a greater propensity for aggregation. Notably, some Span 40 formulations exhibited a statistically significant increase in EE % over time (FS40-4:  $43 \pm 2.3$  % at time 0 to  $64.7 \pm 3.5$  % at 6 months;  $p < 0.01$ ), which may be due to molecular rearrangements within the vesicle bilayer that enhance drug retention, a behavior occasionally reported in the literature (30).

Table V. Stability profile of Span 60 and Span 40 olanzapine niosomal formulations: changes in vesicle size, zeta potential, PDI, and EE % over 6 months at 4–8 °C

Formulation	Time	Particle size (nm)	Zeta potential (mV)	PDI	EE %
FS60-1	Initial	$112 \pm 4$	$-24 \pm 1.6$	$0.31 \pm 0.04$	$81 \pm 2.5$
	3 months	$211.6 \pm 5^*$	$-30.5 \pm 1.5$	$0.29 \pm 0.03$	$76.2 \pm 3$
	6 months	$221.7 \pm 6^*$	$-28.0 \pm 1.6$	$0.37 \pm 0.04$	$74.0 \pm 3.5^*$
FS60-2	Initial	$143 \pm 3.5$	$-27 \pm 1.7$	$0.32 \pm 0.02$	$76 \pm 1.5$
	3 months	$182.1 \pm 4^*$	$-31.3 \pm 1.4$	$0.28 \pm 0.02$	$78.0 \pm 2$
	6 months	$190.7 \pm 5^*$	$-28.7 \pm 1.5$	$0.36 \pm 0.03$	$75.8 \pm 2.5$
FS60-3	Initial	$157 \pm 2.5$	$-33 \pm 2.2$	$0.43 \pm 0.01$	$72 \pm 2.6$
	3 months	$176.7 \pm 3^*$	$-32.0 \pm 1.6$	$0.29 \pm 0.02$	$78.5 \pm 3^*$
	6 months	$185.1 \pm 4^*$	$-29.2 \pm 1.7$	$0.37 \pm 0.03$	$76.2 \pm 3.5^*$
FS60-4	Initial	$168 \pm 9.1$	$-37 \pm 2.8$	$0.38 \pm 0.06$	$70 \pm 2.5$
	3 months	$169.9 \pm 7$	$-32.1 \pm 1.7$	$0.31 \pm 0.03$	$79.2 \pm 3^*$
	6 months	$178.1 \pm 8$	$-29.4 \pm 1.8$	$0.42 \pm 0.04$	$76.8 \pm 3.5^*$
FS40-1	Initial	$180 \pm 18$	$-22 \pm 4$	$0.25 \pm 0.03$	$66 \pm 3.5$
	3 months	$253.3 \pm 20^*$	$-25.6 \pm 1.8$	$0.27 \pm 0.02$	$66.0 \pm 4$
	6 months	$265.5 \pm 22^*$	$-23.0 \pm 1.9$	$0.35 \pm 0.03$	$63.2 \pm 4.5$
FS40-2	Initial	$220 \pm 5.5$	$-24 \pm 4.6$	$0.20 \pm 0.08$	$54 \pm 4$
	3 months	$234.0 \pm 6$	$-26.5 \pm 1.7$	$0.26 \pm 0.03$	$66.7 \pm 4.5^*$
	6 months	$245.3 \pm 7$	$-23.8 \pm 1.8$	$0.34 \pm 0.04$	$63.8 \pm 5$
FS40-3	Initial	$270 \pm 5.2$	$-28 \pm 2.2$	$0.22 \pm 0.03$	$49 \pm 2$
	3 months	$228.3 \pm 6^*$	$-27.1 \pm 1.6$	$0.27 \pm 0.02$	$67.3 \pm 3^*$
	6 months	$239.1 \pm 7^*$	$-24.2 \pm 1.7$	$0.35 \pm 0.03$	$64.3 \pm 3.5^*$
FS40-4	Initial	$310 \pm 30$	$-32 \pm 2.6$	$0.27 \pm 0.07$	$43 \pm 2.3$
	3 months	$220.2 \pm 8^*$	$-27.7 \pm 1.8^*$	$0.26 \pm 0.03$	$67.9 \pm 3^*$
	6 months	$230.7 \pm 9^*$	$-24.6 \pm 1.9^*$	$0.34 \pm 0.04$	$64.7 \pm 3.5^*$

The values are mean  $\pm$  SD,  $n = 3$ . \*Statistically significant difference compared to initial value ( $p < 0.05$ ).

Throughout, PDI values for Span 40 remained  $\leq 0.35$ , indicating acceptable colloidal uniformity.

Collectively, these findings not only confirm that Span 60-based niosomes offer more robust and predictable long-term stability but also reveal the complex and sometimes counterintuitive behaviour of Span 40 systems, where structural changes during storage can unexpectedly enhance drug retention. These results align with literature attributing Span 60's superior stability to its longer alkyl chain and higher phase transition temperature (31), while emphasising the need for tailored stabilisation strategies, particularly optimised storage conditions for Span 40-based formulations intended for sustained-release drug delivery.

## CONCLUSIONS

This study successfully optimised niosomal formulations using Span surfactants and cholesterol, resulting in improved drug encapsulation and a controlled release profile. Among the formulations, Span 60-based niosomes exhibited superior colloidal stability compared to Span 40-based systems, as indicated by smaller increases in vesicle size, more stable surface charge, and better drug retention over time. Nonetheless, the gradual aggregation and drug leakage observed during storage highlight the need for improved stabilisation strategies to ensure long-term integrity. While the findings support the potential of Span 60 niosomes for delivering poorly soluble drugs like olanzapine, further research is required. In particular, comprehensive preclinical studies including evaluations of stability under gastric conditions, permeability, and *in vivo* efficacy are essential. Additionally, clarification of the final dosage form and assessment of formulation scalability will be critical steps toward translating this approach from the laboratory to clinical application.

*Data availability statement.* – The original contributions presented in this study are included in the article. Further inquiries can be directed to the corresponding author.

*Acknowledgements.* – The authors are thankful to the Ongoing Research Funding program (ORF-2025 622), King Saud University, Riyadh, Saudi Arabia, for supporting this work.

*Conflicts of interest.* – The authors declare no conflicts of interest.

*Authors contributions.* – Conceptualization, S.A.; methodology, B.A. and S.A.; formal analysis, G.A.; investigation, S.A. (Shog Alali) and R.K.; resources, L.A. and W.S.; writing, original draft preparation, S.A.; writing, review and editing, B.A., G.A., and N.A. All authors have read and agreed to the published version of the manuscript.

## REFERENCES

1. J. Paik, Olanzapine/Samidorphan: First approval, *Drugs* **81** (2021) 1431–1436; <https://doi.org/10.1007/s40265-021-01568-0>
2. P. Zubiaur, P. Soria-Chacartegui, G. Villalpos-García, J. J. Gordillo-Perdomo and F. Abad-Santos, The pharmacogenetics of treatment with olanzapine, *Pharmacogenomics* **22**(14) (2021) 939–958; <https://doi.org/10.2217/pgs-2021-0051>
3. M. Jovanović, K. Vučićević and B. Miljković, Understanding variability in the pharmacokinetics of atypical antipsychotics – focus on clozapine, olanzapine and aripiprazole population models, *Drug Metab. Rev.* **52**(1) (2020) 1–18; <https://doi.org/10.1080/03602532.2020.1717517>

4. V. Krishnamoorthy, A. Nagalingam, V. P. Ranjan Prasad, S. Parameshwaran, N. George and P. Kailian, Characterization of olanzapine-solid dispersions, *Iran. J. Pharm. Res.* **10**(1) (2011) 13–24; <https://doi.org/10.22037/IJPR.2010.880>
5. J. H. Mao, L. Han, X. Q. Liu and Z. Jiao, Significant predictors for olanzapine pharmacokinetics: A systematic review of population pharmacokinetic studies, *Expert Rev. Clin. Pharmacol.* **16**(6) (2023) 575–588; <https://doi.org/10.1080/17512433.2023.2219055>
6. M. Ur Rehman, A. Rasul, M. I. Khan, M. Rasool, G. Abbas, F. Masood, I. Nazir, M. Iqbal, N. Islam, M. Hameed and P. Akhtar Shah, Oral bioavailability studies of niosomal formulations of cyclosporine A in albino rabbits, *Pak. J. Pharm. Sci.* **34**(1) (2021) 313–319.
7. A. Shahiwal and A. Misra, Studies in topical application of niosomally entrapped nimesulide, *J. Pharm. Pharm. Sci.* **5**(3) (2002) 220–225; <https://pubmed.ncbi.nlm.nih.gov/12553889>
8. P. L. Yeo, C. L. Lim, S. M. Chye, A. P. K. Ling and R. Y. Koh, Niosomes: A review of their structure, properties, methods of preparation, and medical applications, *Asian Biomed.* **11**(4) (2018) 301–314; <https://doi.org/10.1515/abm-2018-0002>
9. Y. K. Lin, C. Y. Hsiao, A. Alshetali, I. A. Aljuffali, E. L. Chen and J. Y. Fang, Lipid-based nanoformulation optimization for achieving cutaneous targeting: Niosomes as the potential candidates to fulfill this aim, *Eur. J. Pharm. Sci.* **186** (2023) Article ID 106458 (13 pages); <https://doi.org/10.1016/j.ejps.2023.106458>
10. M. Moghtaderi, K. Sedaghatnia, M. Bourbour, M. Fatemizadeh, Z. S. M. Moghaddam, F. Hejabi, F. Heidari, S. Quazi and B. Farasati Far, Niosomes: A novel targeted drug delivery system for cancer, *Med. Oncol.* **39** (2022) Article ID 240; <https://doi.org/10.1007/s12032-022-01836-3>
11. D. A. Deulkar, J. A. Kubde, P. R. Hatwar, R. L. Bakal and A. N. Motwani, Niosomes: A promising approach for targeted drug delivery, *GSC Biol. Pharm. Sci.* **29**(1) (2024) 179–195; <https://doi.org/10.30574/gscbps.2024.29.1.0341>
12. S. Gao, Z. Sui, Q. Jiang and Y. Jiang, Functional evaluation of niosomes utilizing surfactants in nanomedicine applications, *Int. J. Nanomedicine* **2024** (2024) 10283–10305; <https://doi.org/10.2147/IJN.5480639>
13. M. Yaghoobian, A. Haeri, N. Bolourchian, S. Shahhosseini and S. Dadashzadeh, The impact of surfactant composition and surface charge of niosomes on the oral absorption of repaglinide as a BCS II model drug, *Int. J. Nanomedicine* **2020** (2020) 8767–8781; <https://doi.org/10.2147/IJN.5261932>
14. B. D. Coday, T. Luxbacher, A. E. Childress, N. Almaraz, P. Xu and T. Y. Cath, Indirect determination of zeta potential at high ionic strength: Specific application to semipermeable polymeric membranes, *J. Memb. Sci.* **478** (2015) 58–64; <https://doi.org/10.1016/j.memsci.2014.12.047>
15. A. K. Sailaja and M. Shreya, Preparation and characterization of naproxen loaded niosomes by ether injection method, *Nano Biomed. Eng.* **10**(2) (2018) 143–149; <https://doi.org/10.5101/nbe.v10i2.p174-180>
16. A. Moammeri, M. M. Chegeni, H. Sahrayi, R. Ghafelehbashi, F. Memarzadeh, A. Mansouri, I. Akbarzadeh, M. Sadat Abtahi, F. Hejabi and Q. Ren, Current advances in niosomes applications for drug delivery and cancer treatment, *Mater. Today Bio.* **23** (2023) Article ID 100837 (20 pages); <https://doi.org/10.1016/j.mtbio.2023.100837>
17. P. Pandey, R. Pal, V. K. R. Khadam, H. S. Chawra and R. P. Singh, Advancement and characteristics of non-ionic surfactant vesicles (niosome) and their application for analgesics, *Int. J. Pharm. Investig.* **14**(3) (2024) 616–632; <https://doi.org/10.5530/IJPI.14.3.74>
18. D. Pozzi, R. Caminiti, C. Marianecchi, M. Carafa, E. Santucci, S. C. De Sanctis and G. Caracciolo, Effect of cholesterol on the formation and hydration behavior of solid-supported niosomal membranes, *Langmuir* **26**(4) (2010) 2268–2273; <https://doi.org/10.1021/la9026877>
19. M. H. Nematollahi, A. Pardakhty, M. Torkzadeh-Mahanai, M. Mehrabani and G. Asadikaram, Changes in physical and chemical properties of niosome membrane induced by cholesterol: A promising approach for niosome bilayer intervention, *RSC Adv.* **7** (2017) Article ID 49463 (10 pages); <https://doi.org/10.1039/C7RA07834J>

20. F. Nowroozi, A. Almasi, J. Javidi, A. Haeri and S. Dadashzadeh, Effect of surfactant type, cholesterol content and various downsizing methods on the particle size of niosomes, *Iran. J. Pharm. Res.* **17** (2018) 1–13.
21. P. Palozza, R. Muzzalupo, S. Trombino, A. Valdannini and N. Picci, Solubilization and stabilization of  $\beta$ -carotene in niosomes: Delivery to cultured cells, *Chem. Phys. Lipids* **139**(1) (2006) 32–42; <https://doi.org/10.1016/j.chemphyslip.2005.09.004>
22. A. Manosroi, P. Wongtrakul, J. Manosroi, H. Sakai, F. Sugawara, M. Yuasa and M. Abe, Characterization of vesicles prepared with various non-ionic surfactants mixed with cholesterol, *Colloids Surf. B Biointerfaces* **30**(1–2) (2003) 129–138; [https://doi.org/10.1016/S0927-7765\(03\)00080-8](https://doi.org/10.1016/S0927-7765(03)00080-8)
23. N. Ruwizhi and B. A. Aderibigbe, The efficacy of cholesterol-based carriers in drug delivery, *Molecules* **25**(18) (2020) Article ID 4330 (40 pages); <https://doi.org/10.3390/molecules25184330>
24. N. S. Heredia, K. Vizuite, M. Flores-Calero, V. Pazmiño, F. K. Pilaquinga, B. Kumar and A. Debut, Comparative statistical analysis of the release kinetics models for nanoprecipitated drug delivery systems based on poly(lactic-co-glycolic acid), *PLoS One* **17** (2022) e0264825 (18 pages); <https://doi.org/10.1371/journal.pone.0264825>
25. I. Y. Wu, S. Bala, N. Škalko-Basnet and M. P. di Cagno, Interpreting non-linear drug diffusion data: Utilizing Korsmeyer-Peppas model to study drug release from liposomes, *Eur. J. Pharm. Sci.* **138** (2019) Article ID 105026 (14 pages); <https://doi.org/10.1016/j.ejps.2019.105026>
26. S. Zolghadri, A. G. Asad, F. Farzi, F. Ghajarzadeh, Z. Habibi, M. Rahban, S. Zolghadri and A. Stanek, Span 60/cholesterol niosomal formulation as a suitable vehicle for gallic acid delivery with potent in vitro antibacterial, antimelanoma, and antityrosinase activity, *Pharmaceuticals* **16**(12) (2023) Article ID 1680; <https://doi.org/10.3390/ph16121680>
27. B. Korchowiec, M. Paluch, Y. Corvis and E. Rogalska, A Langmuir film approach to elucidating interactions in lipid membranes: 1,2-dipalmitoyl-*sn*-glycero-3-phosphoethanolamine/cholesterol/metal cation systems, *Chem. Phys. Lipids* **144**(2) (2006) 127–136; <https://doi.org/10.1016/j.chemphyslip.2006.08.005>
28. A. Rasul, M. Imran Khan, M. U. Rehman, G. Abbas, N. Aslam, S. Ahmad, K. Abbas, P. Akhtar Shah, M. Iqbal, A. M. Ahmed Al Subari, T. Shaheer and S. Shas, In vitro characterization and release studies of combined nonionic surfactant-based vesicles for the prolonged delivery of an immunosuppressant model drug, *Int. J. Nanomedicine* **2020** (2020) 7937–7949; <https://doi.org/10.2147/IJN.S268846>
29. M. H. Mowlaeifar, M. Niakousari, S. M. H. Hosseini and M. H. Eskandari, Effect of cholesterol to vitamin D3 and Span 60 to Tween 60 ratios on the characteristics of niosomes: Variable optimization using response surface methodology (RSM), *J. Food Qual.* **2022** (2022) Article ID 7005531 (8 pages); <https://doi.org/10.1155/2022/7005531>
30. G. Abdelbary and N. El-gendy, Niosome-encapsulated gentamicin for ophthalmic controlled delivery, *AAPS PharmSciTech* **9** (2008) 740–747; <https://doi.org/10.1208/s12249-008-9105-1>
31. P. Balakrishnan, B. J. Lee, D. H. Oh, J. O. Kim, Y. I. Lee, D. D. Kim, J.-P. Jee, Y.-B. Lee, J. S. Woo, C. S. Yong and H.-G. Choi, Enhanced oral bioavailability of Coenzyme Q10 by self-emulsifying drug delivery systems, *Int. J. Pharm.* **374**(1–2) (2009) 66–72; <https://doi.org/10.1016/j.ijpharm.2009.03.008>